

Edge Excitations in Fractional Chern Insulators

Wei-Wei Luo¹, Wen-Chao Chen¹, Yi-Fei Wang¹, Chang-De Gong^{1,2}

¹*Center for Statistical and Theoretical Condensed Matter Physics,
and Department of Physics, Zhejiang Normal University, Jinhua 321004, China*

²*National Laboratory of Solid State Microstructures and Department of Physics, Nanjing University, Nanjing 210093, China*

(Dated: April 17, 2013)

Recent theoretical works have demonstrated the realization of fractional quantum anomalous Hall states (also called fractional Chern insulators) in topological flat band lattice models without an external magnetic field. Such newly proposed lattice systems with topological flat bands play a vital role to obtain a large class of fractional topological phases. Here we report the exact numerical studies of edge excitations for such systems in a disk geometry loaded with hard-core bosons, which will serve as a more viable experimental probe for such new fractional topological phases. We find convincing numerical evidence of a series of edge excitations characterized by the chiral Luttinger liquid theory for the bosonic fractional Chern insulators in both the honeycomb disk Haldane model and the kagomé-lattice disk model. We further verify these current-carrying chiral edge states by inserting a central flux to test their compressibility.

PACS numbers: 73.43.Cd, 05.30.Jp, 71.10.Fd, 37.10.Jk

Introduction.— One of the most essential and fascinating topics in condensed matter physics is to explore and classify the various states of matter, among which the integer quantum Hall effect (IQHE) [1] and the fractional quantum Hall effect (FQHE) [2] have long been the major focus. It is well known that, at fractional fillings, the FQHE will emerge when interacting particles move in Landau levels (LLs) caused by an external uniform magnetic field. On the other hand, great interest has been aroused to realize both the IQHE and FQHE in lattice models in the absence of an external magnetic field. An initial theoretical attempt was made by Haldane [3], who proposed a prototype lattice model to achieve the IQHE by introducing two non-trivial topological bands with Chern numbers $C = \pm 1$ [4]. Haldane's model demonstrates that the IQHE can also be attained without LLs, i.e. defines the quantum anomalous Hall (QAH) states. The lattice version of the FQHE without LLs, however, comes much latter because of its intriguing strongly correlated nature.

The recent proposal of topological flat bands (TFBs) fulfils the basic ingredients to explore the intriguing fractionalization phenomenon without LLs. TFBs [5–7] belong to a class of band structures with at least one nearly flat band with non-zero Chern number. This may be viewed as the lattice counterpart of the continuum LLs. Several systematic numerical works have been done to explore the correlation phenomenon within TFB models, and Abelian [8–10] and non-Abelian [11–13] FQHE states without LLs have already been well established numerically. This intriguing fractionalization effect in TFBs without an external magnetic field, defines a new class of fractional topological phases, i.e. fractional quantum anomalous Hall (FQAH) states, now also known as fractional Chern insulators (FCIs). Some new approaches, e.g. the Wannier-basis model wave functions and pseudo-potentials [14], the projected density opera-

tor algebra [15], the parton wave-function constructions [16], and also the adiabatic continuity paths [17], have been proposed to further understand these FCI/FQAH states in TFBs. There are various other proposals of TFB models and material realization schemes [18–34]. Very recent systematic numerical studies have also found exotic FCI/FQAH states in TFBs with higher Chern numbers ($C \geq 2$) which do not have the direct continuum analogy in LLs [35–37], and also the hierarchy FCI/FQAH states [38].

Although previous studies have firmly established various properties of a large class of FCI/FQAH phases, we are here concerned with the less studied edge excitations since they in principle should open another window to reveal the bulk topological order [39]. Edge excitations might also provide a more viable experimental probe [40] especially considering about the possible future realizations of FCI/FQAH phases in optical lattice systems [30]. A recent work has studied edge excitations of the bosonic FQHE in LLs generated by an artificial uniform flux in optical lattices [41]. In the present work, we investigate edge excitations of the bosonic FCI/FQAH phases [9] of TFB models in a disk geometry. Through extensive systematic numerical exact diagonalization (ED) studies, we demonstrate clear evidence of edge excitation spectra of bosonic FCI/FQAH phases. These edge excitation spectra are quite coincident with the chiral Luttinger liquid theory [39]. To further check the compressibility of these edge states, we insert a central flux into the disk system and indeed verify these current-carrying chiral edge states upon tuning the flux strength.

Model Hamiltonians.— We first look into the Haldane model [3] on a honeycomb-lattice disk, which is loaded

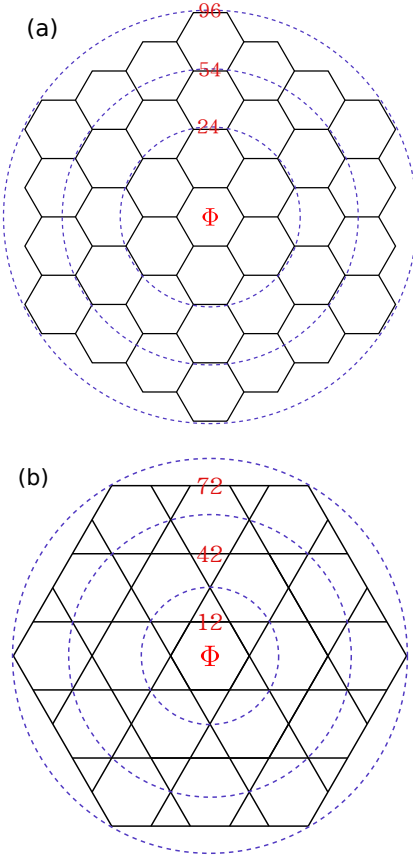


FIG. 1: (color online). (a) The honeycomb-lattice disk and (b) the kagomé-lattice disk. Both disk geometries satisfy the C_6 rotational symmetry. Various disk sizes are indicated by the circles and the labelled numbers.

with interacting hard-core bosons [9]:

$$H_{\text{HC}} = -t' \sum_{\langle\langle \mathbf{r} \mathbf{r}' \rangle\rangle} [b_{\mathbf{r}'}^\dagger b_{\mathbf{r}} \exp(i\phi_{\mathbf{r}'\mathbf{r}}) + \text{H.c.}] \quad (1)$$

$$-t \sum_{\langle \mathbf{r} \mathbf{r}' \rangle} [b_{\mathbf{r}'}^\dagger b_{\mathbf{r}} + \text{H.c.}] - t'' \sum_{\langle\langle\langle \mathbf{r} \mathbf{r}' \rangle\rangle\rangle} [b_{\mathbf{r}'}^\dagger b_{\mathbf{r}} + \text{H.c.}]$$

where $b_{\mathbf{r}}^\dagger$ creates a hard-core boson at site \mathbf{r} , $\langle \dots \rangle$, $\langle \langle \dots \rangle \rangle$ and $\langle \langle \langle \dots \rangle \rangle \rangle$ denote the NN, the NNN and the next-nearest-neighbor (NNNN) pairs of sites, respectively. We adopt the previous parameters [9] to achieve a lowest TFB with a flatness ratio of about 50 (the ratio of the band gap over bandwidth): $t = 1$, $t' = 0.60$, $t'' = -0.58$ and $\phi = 0.4\pi$.

We also consider a kagomé lattice TFB model [5, 25] which is also loaded with hard-core bosons, and the model Hamiltonian has the form:

$$H_{\text{KG}} = -t \sum_{\langle \mathbf{r} \mathbf{r}' \rangle} [b_{\mathbf{r}'}^\dagger b_{\mathbf{r}} \exp(i\phi_{\mathbf{r}'\mathbf{r}}) + \text{H.c.}] \quad (2)$$

$$-t' \sum_{\langle\langle \mathbf{r} \mathbf{r}' \rangle\rangle} [b_{\mathbf{r}'}^\dagger b_{\mathbf{r}} + \text{H.c.}]$$

We choose the previous parameters for this kagomé-lattice model [25]: $t = 1$, $t' = -0.19$, $\phi = 0.22\pi$, which leads to a lowest TFB with the flatness ratio of about 20.

Convincing numerical evidence of the 1/2 bosonic FCI/FQAH states at the 1/2 hard-core boson filling of a lowest TFB on a torus geometry has been well established previously [9], with the formation of a quasi-degenerate ground-state (GS) manifold, characteristic GS momenta, a robust bulk excitation spectrum gap, as well as a fractional quantized Chern number for each GS. The disk geometries for both lattice models are illustrated in Fig. 1, which shows the C_6 rotational symmetry. An additional trap potential is required on the finite-size disk systems to confine the FCI/FQAH droplet, outside which the edge modes are able to propagate around the disk. Here we choose the conventional harmonic trap, of the form $V = V_{\text{trap}} \sum_{\mathbf{r}} |\mathbf{r}|^2 n_{\mathbf{r}}$ with V_{trap} as the potential strength, $|\mathbf{r}|$ as the radius from the disk center, and $n_{\mathbf{r}}$ as the boson number operator.

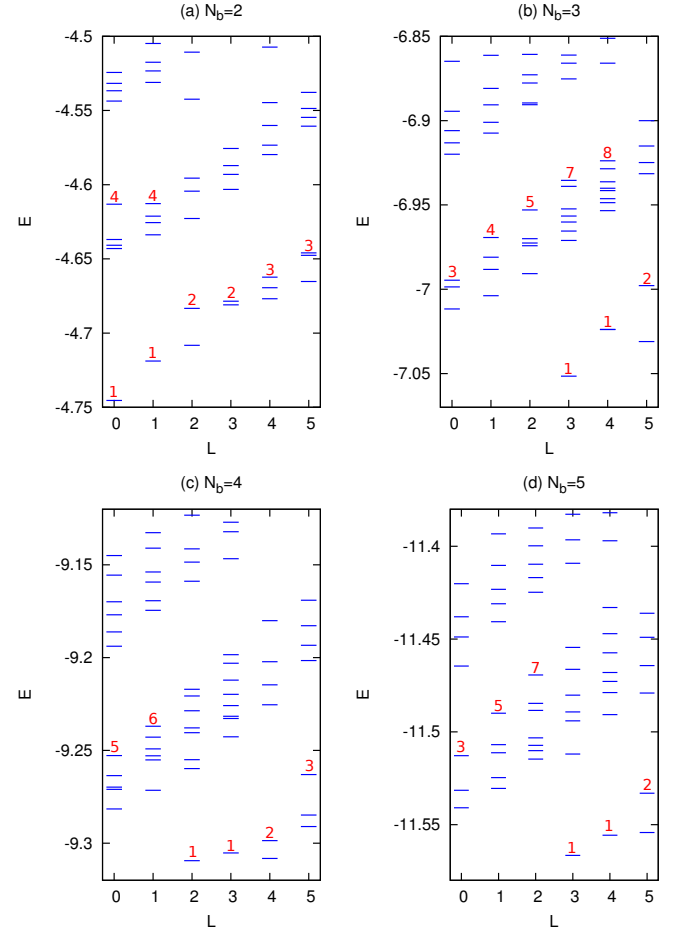


FIG. 2: (color online). Edge excitations on a honeycomb disk with $N_s = 96$ sites and trap potential $V_{\text{trap}} = 0.005$. Numbers labelled upon low energy levels in each sector show the quasi-degeneracy of low edge excitations, which is also the sequence derived from the chiral Luttinger liquid theory.

Edge excitations.— We have first considered the honeycomb disk model, and have observed clear edge excitation spectra for a relative broad range of the trap potential strength V_{trap} and various honeycomb disk sizes with $N_s = 24, 54, 96$ sites. Some representative results are shown in Fig. 2. As the system owns the C_6 rotational symmetry, each energy states can be classified with a quantum number of angular momentum $L = 0, 1, 2, 3, \dots$, mod 6. These edge-excitation quasi-degeneracies of a finite system with various boson numbers turn out to be a good match with that predicted by the chiral Luttinger liquid theory at least for the lowest six sectors.

ΔL	$\{n_1, n_2, n_3, n_4, n_5, n_6, \dots\}$	2b 3b 4b 5b 6b
0	$\{0,0,0,0,0,0, \dots\}$	$d = 1 \ 1 \ 1 \ 1 \ 1$
1	$\{1,0,0,0,0,0, \dots\}$	$d = 1 \ 1 \ 1 \ 1 \ 1$
2	$\{0,1,0,0,0,0, \dots\}, \{2,0,0,0,0,0, \dots\}$	$d = 2 \ 2 \ 2 \ 2 \ 2$
3	$\{0,0,1,0,0,0, \dots\}, \{1,1,0,0,0,0, \dots\}$ $\{3,0,0,0,0,0, \dots\}$	$d = 2 \ 3 \ 3 \ 3 \ 3$
4	$\{0,0,0,1,0,0, \dots\}, \{1,0,1,0,0,0, \dots\}$ $\{0,2,0,0,0,0, \dots\}, \{2,1,0,0,0,0, \dots\}$ $\{4,0,0,0,0,0, \dots\}$	$d = 3 \ 4 \ 5 \ 5 \ 5$
5	$\{0,0,0,0,1,0, \dots\}, \{1,0,0,1,0,0, \dots\}$ $\{0,1,1,0,0,0, \dots\}, \{2,0,1,0,0,0, \dots\}$ $\{1,2,0,0,0,0, \dots\}, \{3,1,0,0,0,0, \dots\}$ $\{5,0,0,0,0,0, \dots\}$	$d = 3 \ 5 \ 6 \ 7 \ 7$
6	$\{0,0,0,0,0,1, \dots\}, \{1,0,0,0,1,0, \dots\}$ $\{0,1,0,1,0,0, \dots\}, \{2,0,0,1,0,0, \dots\}$ $\{0,0,2,0,0,0, \dots\}, \{1,1,1,0,0,0, \dots\}$ $\{3,0,1,0,0,0, \dots\}, \{0,3,0,0,0,0, \dots\}$ $\{2,2,0,0,0,0, \dots\}, \{4,1,0,0,0,0, \dots\}$ $\{6,0,0,0,0,0, \dots\}$	$d = 4 \ 7 \ 9 \ \underline{10} \ \underline{11}$

TABLE I: Occupation of chiral edge bosons in $k = 1, 2, 3, 4, 5, 6, \dots$ orbitals: $\{n_1, n_2, n_3, n_4, n_5, n_6, \dots\}$. d is the degeneracy of the edge excitations in a sector. $\Delta L = L - L_{\text{GS}} = \sum_k k n_k$, which is the shifted total angular momentum relative to the ground state angular momentum. The right column shows the degeneracy in systems with finite boson numbers, e.g., for the “4b” column ($N_b = 4$), the predicted degeneracy is $1, 1, 2, 3, 5, 6, 9, \dots$ in $\Delta L = 0, 1, 2, 3, 4, 5, 6, \dots$ angular momentum sectors. The partial degeneracy sequences are mostly observed (except the underlined 9, 10 and 11) in our ED results.

According to the hydrodynamical approach [39], low energy edge excitations of a Laughlin-state FQHE droplet at filling $\nu = 1/m$ are generated by the Kac-Moody algebra, and form a chiral Luttinger liquid with the effective Hamiltonian:

$$H_{1/m} = 2\pi \frac{v}{\nu} \sum_{k>0} \rho_{-k} \rho_k = v \sum_{k>0} k a_k^\dagger a_k, \quad (3)$$

with the angular momentum k along the edge and the Fourier-transformed one-dimensional density opera-

tor ρ_k , $[\rho_k, \rho_{k'}] = \frac{\nu}{2\pi} k \delta_{k+k'}$, a_k^\dagger and a_k are chiral boson/phonon operators. Based on this theory, chiral edge bosons occupy in $k = 1, 2, 3, 4, 5, 6, \dots$ (unit $2\pi/M$ and edge length M) angular momentum orbitals with the occupation numbers $\{n_1, n_2, n_3, n_4, n_5, n_6, \dots\}$. We denote $\Delta L = L - L_{\text{GS}}$ as the shifted total angular momentum relative to the GS angular momentum. For a given $\Delta L = \sum_k k n_k$, it is easy to count the edge-state degeneracies by numerating the allowed occupation configurations. In the thermodynamics limit with infinite boson numbers, the degeneracy sequence should be $1, 1, 2, 3, 5, 7, 11, 15, 22, \dots$. For our systems with only small boson number N_b ’s, edge excitations made up of $\sum_k n_k \leq N_b$ single modes are expected. For three bosons ($N_b = 3$), after discarding some configurations in the middle column of Table I with $\sum_k n_k > N_b = 3$, the predicted degeneracy should be $1, 1, 2, 3, 4, 5, 7, \dots$, which is in good accordance with the observed quasi-degeneracy in our ED results [Fig. 2(b)]. For four bosons ($N_b = 4$), after discarding some configurations with $\sum_k n_k > N_b = 4$, the predicted degeneracy should be $1, 1, 2, 3, 5, 6, \dots$, which is also in good accordance with the observed quasi-degeneracy in our ED results [Fig. 2(c)]. The right column in Table I list the partial degeneracy sequences which are mostly observed in our ED results.

Now we turn to investigate the kagomé disk model. We studied the finite system also in several different sizes, with $N_s = 12, 30, 42, 72$ sites. Edge spectra from a finite kagomé disk with $N_s = 72$ sites are shown in Fig. 3, which shows even clearer edge excitation spectra than that obtained from $N_s = 96$ honeycomb disk. It is quite exciting to observe that these edge excitations are independent of lattice geometry even in such small systems. For an example with six bosons ($N_b = 6$), after discarding some states with $\sum_k n_k > N_b = 6$, the predicted degeneracy should be $1, 1, 2, 3, 5, 7, \dots$ which is also in exact accordance with the observed quasi-degeneracy in our ED results [Fig. 3(d)]. It is also observed that with the larger disk sizes and smaller boson numbers, the number of matched momentum sectors increases, and thus displays less severe finite size effects.

Central flux.—As a next step, we insert a flux into the center of disk geometry and tune the flux strength to test the compressibility of edge excitations. Consider the kagomé disk with $N_s = 42$ sites for an example; the trap potential will always be fixed as $V_{\text{trap}} = 0.005$. For systems with $N_b = 3$ bosons, low energy levels E_n in $k = 0, 3$ sectors (or $k = 1, 4$ and $k = 2, 5$ sectors) evolve into each other, as is shown in Fig. 4(a). These energy spectra E_n finally return to themselves after two periods of the central flux, i.e. $E_n(\Phi + 4\pi) = E_n(\Phi)$. For systems with $N_b = 4$ bosons, low energy levels E_n in $k = 0, 2, 4$ sectors (or $k = 1, 3, 5$ sectors) evolve into each other, as is shown in Fig. 4(b). These states finally return to themselves after three periods of the central flux, i.e. $E_n(\Phi + 6\pi) = E_n(\Phi)$. For our disk

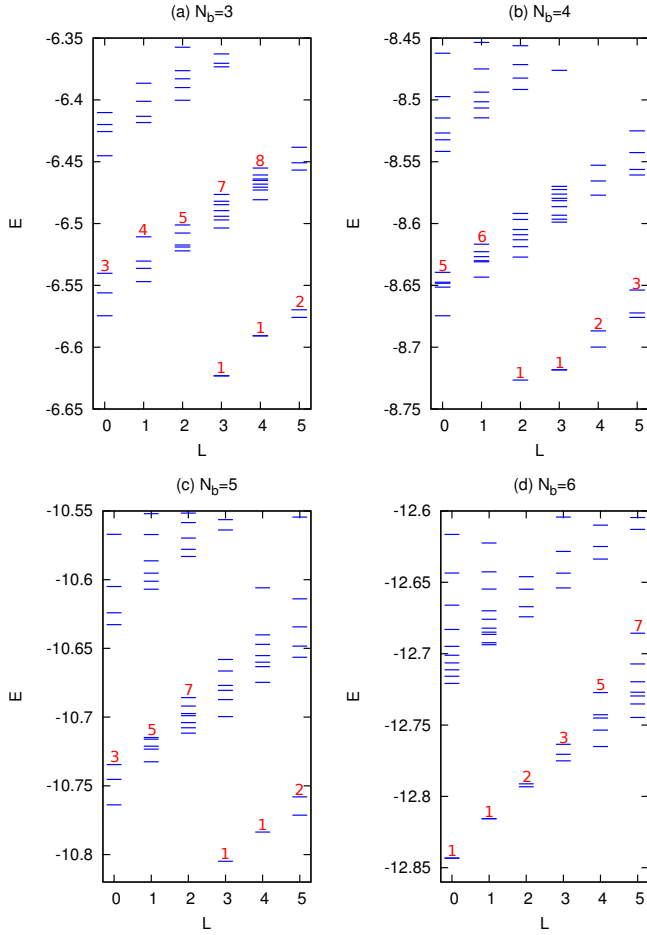


FIG. 3: (color online). Edge excitations on a kagomé disk with $N_s = 72$ sites and trap potential $V_{\text{trap}} = 0.005$. Numbers labelled upon low energy levels in each sector show the quasi-degeneracy of low edge excitations, which is also the sequence derived from the chiral Luttinger liquid theory.

systems with the C_6 rotational symmetry, when boson numbers satisfy $N_b/6 = p/q$ with p and q as coprime integers, there is a generic periodicity of energy spectra: $E_n(\Phi + 2q\pi) = E_n(\Phi)$. It is obvious to observe the current-carrying nature, i.e. the compressibility of edge states since all of them evolve into the higher energy spectra without any gap. These low edge excitations are in principal all degenerate in the thermodynamic limit, as is explained in the microscopic theory of FQHE droplet. When the boson numbers increases in the disk system, mixture of bulk topological insulating states become apparent. For the system with $N_s = 42$ sites and $N_b = 6$ bosons, we thus get an incompressible ground state, which is always gapped from other excited states as shown in Fig. 4(c).

Summary and discussion.—We considered two representative TFB lattice models in disk geometry to explore edge excitations of FCI/FQAH states. With a confining harmonic trap potential, very clear edge excitation

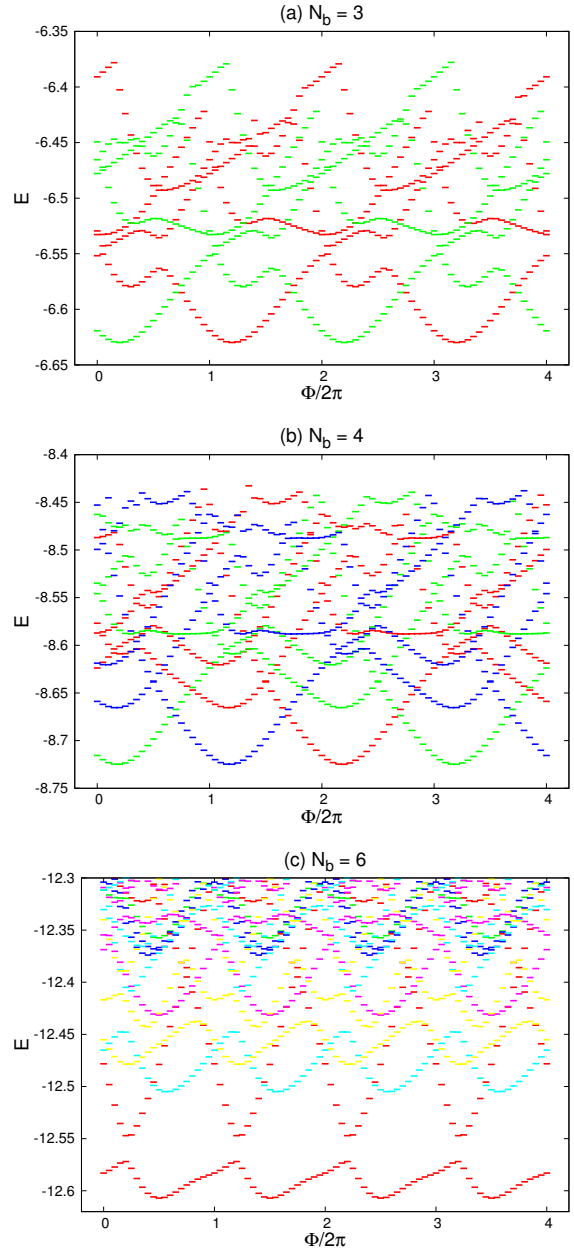


FIG. 4: (color online). Evolution of low energy states with the varying central flux of the kagomé disk with $N_s = 42$ sites, trap potential $V_{\text{trap}} = 0.005$, and various boson numbers N_b 's. (a) For $N_b = 3$, low energy states in $k = 0, 3$ sectors (red, green respectively) evolve into each other. (b) For $N_b = 4$, low energy states in $k = 0, 2, 4$ sectors (red, green, blue respectively) evolve into each other. (c) For $N_b = 6$, low energy states in all six sectors are displayed, and the ground state is gapped from other excited states, showing the incompressible nature of an insulating state.

spectra are observed with the quasi-degeneracy counting rule satisfying the chiral Luttinger liquid theory at least for the lowest six sectors. By inserting and tuning a central flux to both systems, we are able to examine the compressibility of these current-carrying chiral edge

states. Our work here focuses on the bosonic FCI/FQAH states in TFBs with the Chern number $C = 1$, while it is very interesting to explore the exotic edge excitations in high-Chern-number FCI/FQAH phases [35–37] and also those in the hierarchy FCI/FQAH phases [38] in future works. We also expect that edge excitation spectra provide another window to reveal the bulk topological order, as well as a more viable experimental probe to future FCI/FQAH experimental systems.

We acknowledge Prof. D. N. Sheng for helpful discussions and previous collaborations. This work is supported by the NSFC of China Grants No. 10904130 (Y.F.W.) and No. 11274276 (C.D.G.), and the State Key Program for Basic Researches of China Grant No. 2009CB929504 (C.D.G.).

[1] K. v. Klitzing, G. Dorda, and M. Pepper, Phys. Rev. Lett. **45**, 494 (1980).

[2] D. C. Tsui, H. L. Stormer, and A. C. Gossard, Phys. Rev. Lett. **48**, 1559 (1982).

[3] F. D. M. Haldane, Phys. Rev. Lett. **61**, 2015 (1988).

[4] D. J. Thouless, M. Kohmoto, M. P. Nightingale, and M. den Nijs, Phys. Rev. Lett. **49**, 405 (1982).

[5] E. Tang, J. W. Mei, and X. G. Wen, Phys. Rev. Lett. **106**, 236802 (2011).

[6] K. Sun, Z. C. Gu, H. Katsura, and S. Das Sarma, Phys. Rev. Lett. **106**, 236803 (2011).

[7] T. Neupert, L. Santos, C. Chamon, and C. Mudry, Phys. Rev. Lett. **106**, 236804 (2011).

[8] D. N. Sheng, Z. C. Gu, K. Sun, and L. Sheng, Nature Commun. **2**, 389 (2011).

[9] Y. F. Wang, Z. C. Gu, C. D. Gong, and D. N. Sheng, Phys. Rev. Lett. **107**, 146803 (2011).

[10] N. Regnault and B. A. Bernevig, Phys. Rev. X **1**, 021014 (2011).

[11] Y. F. Wang, H. Yao, Z. C. Gu, C. D. Gong, and D. N. Sheng, Phys. Rev. Lett. **108**, 126805 (2012).

[12] B. A. Bernevig and N. Regnault, Phys. Rev. B **85**, 075128 (2012).

[13] Y. L. Wu, B. A. Bernevig, and N. Regnault, Phys. Rev. B **85**, 075116 (2012).

[14] X. L. Qi, Phys. Rev. Lett. **107**, 126803 (2011); M. Barkeshli and X. L. Qi, Phys. Rev. X **2**, 031013 (2012); Y. L. Wu, N. Regnault, and B. A. Bernevig, Phys. Rev. Lett. **110**, 106802 (2013); C. H. Lee, R. Thomale, X. L. Qi, arXiv:1207.5587; C. M. Jian and X. L. Qi, arXiv:1303.1787.

[15] S. A. Parameswaran, R. Roy, and S. L. Sondhi, Phys. Rev. B **85**, 241308 (2012); M. O. Goerbig, Eur. Phys. J. B **85**, 15 (2012). G. Murthy and R. Shankar, arXiv:1108.5501; G. Murthy and R. Shankar, Phys. Rev. B **86**, 195146 (2012).

[16] Y. M. Lu and Y. Ran, Phys. Rev. B **85**, 165134 (2012); J. McGreevy, B. Swingle, and K. A. Tran, Phys. Rev. B **85**, 125105 (2012); A. Vaezi, arXiv:1105.0406; Y. Zhang and A. Vishwanath, arXiv:1209.2424

[17] T. Scaffidi and G. Möller, Phys. Rev. Lett. **109**, 246805 (2012); Y. H. Wu, J. K. Jain, and K. Sun, Phys. Rev. B **86**, 165129 (2012).

[18] X. Hu, M. Kargarian, and G. A. Fiete, Phys. Rev. B **84**, 155116 (2011).

[19] D. Xiao, W. Zhu, Y. Ran, N. Nagaosa, and S. Okamoto, Nature Commun. **2**, 596 (2011).

[20] J. W. F. Venderbos, M. Daghofer, and J. van den Brink, Phys. Rev. Lett. **107**, 116401 (2011).

[21] P. Ghaemi, J. Cayssol, D. N. Sheng, and A. Vishwanath, Phys. Rev. Lett. **108**, 266801 (2012).

[22] F. Wang and Y. Ran, Phys. Rev. B **84**, 241103(R) (2011).

[23] J. W. F. Venderbos, S. Kourtis, J. van den Brink, and M. Daghofer, Phys. Rev. Lett. **108**, 126405 (2012).

[24] C. Weeks, and M. Franz, Phys. Rev. B **85**, 041104(R) (2012).

[25] R. Liu, W. C. Chen, Y. F. Wang, and C. D. Gong, J. Phys.: Condens. Matter **24**, 305602 (2012).

[26] W. C. Chen, R. Liu, Y. F. Wang, C. D. Gong, Phys. Rev. B **86**, 085311 (2012).

[27] M. Trescher and E. J. Bergholtz, Phys. Rev. B **86**, 241111(R) (2012).

[28] S. Yang, Z. C. Gu, K. Sun, and S. Das Sarma, Phys. Rev. B **86**, 241112(R) (2012).

[29] A. G. Grushin, T. Neupert, C. Chamon, and C. Mudry, Phys. Rev. B **86**, 205125 (2012).

[30] N.Y. Yao, C.R. Laumann, A.V. Gorshkov, S.D. Bennett, E. Demler, P. Zoller, and M.D. Lukin, Phys. Rev. Lett. **109**, 266804 (2012); N. Y. Yao, A. V. Gorshkov, C. R. Laumann, A. M. Läuchli, J. Ye, M. D. Lukin, arXiv:1212.4839.

[31] V. Yannopapas, New J. Phys. **14**, 113017 (2012).

[32] Y. Zhang and C. Zhang, Phys. Rev. A **87**, 023611 (2013).

[33] Z. Liu, Z. F. Wang, J. W. Mei, Y. S. Wu, and F. Liu, Phys. Rev. Lett. **110**, 106804 (2013).

[34] T. Shi and J. I. Cirac, Phys. Rev. A **87**, 013606 (2013).

[35] Y. F. Wang, H. Yao, C. D. Gong, and D. N. Sheng, Phys. Rev. B **86**, 201101(R) (2012).

[36] Z. Liu, E. J. Bergholtz, H. Fan, and A. M. Läuchli, Phys. Rev. Lett. **109**, 186805 (2012).

[37] A. Sterdyniak, C. Repellin, B. A. Bernevig, and N. Regnault, arXiv:1207.6385.

[38] T. Liu, C. Repellin, B. A. Bernevig, and N. Regnault, arXiv:1206.2626; A. M. Läuchli, Z. Liu, E. J. Bergholtz, and R. Moessner, arXiv:1207.6094.

[39] X. G. Wen, Adv. Phys. **44**, 405 (1995).

[40] T. D. Stanescu, V. Galitski, J. Y. Vaishnav, C. W. Clark, and S. Das Sarma, Phys. Rev. A **79**, 053639 (2009); N. Goldman, J. Beugnon, and F. Gerbier, Phys. Rev. Lett. **108**, 255303 (2012).

[41] J. A. Kjäll and J. E. Moore, Phys. Rev. B **85**, 235137 (2012).